Changes in the substructure of tempered martensitic steel during the application of cyclic elastic stress in the presence of hydrogen

M Ohori[1], T Chiba[1], Y Matsumoto[1], H Suzuki[2] and K Takai[2]

[1]Graduate School of Science and Technology, Sophia University, 7-1 Kioi-cho, Chiyoda-ku, Tokyo 102-8554, Japan
[2]Faculty of Science and Technology, Department of Engineering and Applied Sciences, Sophia University, Tokyo, Japan

Corresponding author's e-mail address: m-ohori-3wr@eagle.sophia.ac.jp

Abstract. Changes in the substructure of tempered martensitic steel during the application of cyclic elastic stress in the presence of hydrogen have been investigated. Three types of specimens were prepared. The first type was subjected to cyclic elastic stress (strain rate: 3.0×10^{-4} s^{-1}, number of cycles: 70000, and stress level: 0.8±0.1 σ_B) without hydrogen. The second type was subjected to cyclic elastic stress with hydrogen. The third type was prepared by annealing the second type at 200 ℃ for 2 h. These specimens are denoted here as [(n)-cycled], [H+(n)-cycled] and [H+(n)-cycled+annealed] specimens, respectively. Tracer hydrogen was used as a probe for clarifying changes in the specimen substructure. After tracer hydrogen charging, hydrogen states present in the specimens were examined using low-temperature thermal desorption spectrometry (L-TDS). Tracer hydrogen desorption in the high-temperature range from the [H+(n)-cycled] specimen increased compared with that from the [(n)-cycled] specimen. In addition, tracer hydrogen desorption in the high-temperature range from the [H+(n)-cycled+annealed] specimen was reduced by annealing at 200 ℃ to the level of the [(n)-cycled] specimen. As a result, it is inferred that the formation of vacancy type defects was enhanced under the application of cyclic elastic stress in the presence of hydrogen.

1 Introduction

Hydrogen is trapped at various trapping sites in steels. The degree of influence of hydrogen on hydrogen embrittlement differs among the different kinds of trapping sites. In previous studies, the formation of vacancy-type defects in the vicinity of the fracture surface of specimens that were fractured under constant elastic tensile stress with hydrogen has been reported for tempered martensitic steels [1]. Furthermore, it has also been reported that plastic deformation with hydrogen increased the formation of vacancy-type defects [2]. Vacancy-type defects have been reported to cause degradation of mechanical properties such as ductility loss. However, steels are subjected not only to constant elastic stress but also to cyclic stress in actual environments. Accordingly, it is imperative to clarify the changes in the substructure of steels during the application of cyclic elastic stress in the presence of hydrogen. In terms of fatigue behavior, the effects of hydrogen on fatigue crack propagation [3] and cyclic hardening/softening [4] under cyclic loading with hydrogen have been reported. On a contrary, there have been few reports regarding the effects of hydrogen on substructure changes before the occurrence of damage such as crack formation. Correspondingly, in this study, we

investigated changes in the substructure of tempered martensitic steel during the application of cyclic elastic stress with hydrogen.

2 Experimental

2.1 Materials

The chemical composition of the tempered martensitic steel specimens used in this study is listed in Table 1. The specimens were induction quenched at 960 °C and tempered at 360 °C. The tensile strength (σ_B) and proof stress of 0.2% were 1471 MPa and 1384 MPa, respectively. Figure 1 displays the specimen shape having a diameter of 5 mm and a gauge length of 30 mm.

2.2 Hydrogen precharging conditions

Prior to hydrogen precharging, the specimen surface was mechanically polished using emery papers (#800, 1000 and 2000). The specimens were charged electrochemically with hydrogen at a current density of 10 $A \cdot m^{-2}$ in a 4 $g \cdot L^{-1}$ N NaOH aqueous solution kept at 30 °C and containing a NH_4SCN additive of 1 $g \cdot L^{-1}$. The charging time was 72 h to reach an equilibrium hydrogen concentration at both the surface and the center of the specimens. These charging conditions provided the equilibrium hydrogen concentration of approximately 2.6 mass ppm in the specimens.

2.3 Preparation of specimens subjected to cyclic elastic stress

Three types of specimens subjected to cyclic elastic stress with/without hydrogen were prepared. The applied cyclic elastic stress was a triangular wave at 0.8±0.1 σ_B. The strain rate during cyclic elastic stress was 3.0×10^{-4} s^{-1}. The numbers of cycles (n) were 700, 7000 and 70000. The first type, denoted as the [(n)-cycled] specimens, was subjected to cyclic elastic stress at 30 °C without hydrogen. The second type, denoted as the [H+(n)-cycled] specimens, was subjected to cyclic elastic stress at 30 °C with hydrogen. The third type, denoted as the [H+(n)-cycled+annealed] specimens, was obtained by annealing the second type at 200 °C for 2 h. The second and third specimen types were precharged with hydrogen and then cyclic elastic stress was applied concurrently with hydrogen charging for maintaining the hydrogen content of the specimens.

2.4 Tracer hydrogen charging and hydrogen analysis

Figure 2 shows a schematic diagram of the applied cyclic elastic stress and subsequent L-TDS. After the application of cyclic elastic stress, the specimens were aged for 5 days in air at 30 °C to completely degas the absorbed hydrogen. The specimens were then cut to 1 mm in gauge length for hydrogen analysis. The deformation layer on the specimen surface of all three types was removed by mechanical polishing followed by chemical polishing, which reduced the specimen thickness to 0.2 mm. Hydrogen was used as a tracer to clarify the changes in the specimen substructure during the application of cyclic elastic stress with hydrogen. Tracer hydrogen was charged into the specimens by immersion for 24 h in a 0.5 $g \cdot L^{-1}$ NH_4SCN solution kept at 30 °C. The specimens were then immediately immersed in liquid nitrogen to prevent the release of hydrogen. States of hydrogen were examined using low-temperature thermal desorption spectroscopy (L-TDS), which can heat specimens from lower temperatures than conventional TDS. The specimens were then mounted on the heating stage of the L-TDS equipment and heated at a rate of 1 °C/min from –200 to 200 °C.

Table 1. Chemical composition of specimens (mass %)

C	Si	Mn	P	S
0.34	0.27	0.80	0.012	0.008

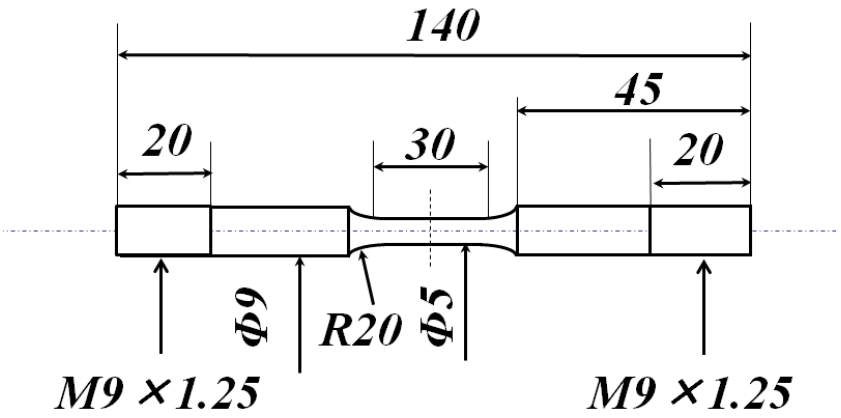

Figure 1. Geometry and dimensions (in mm) of the specimens subjected to cyclic elastic stress

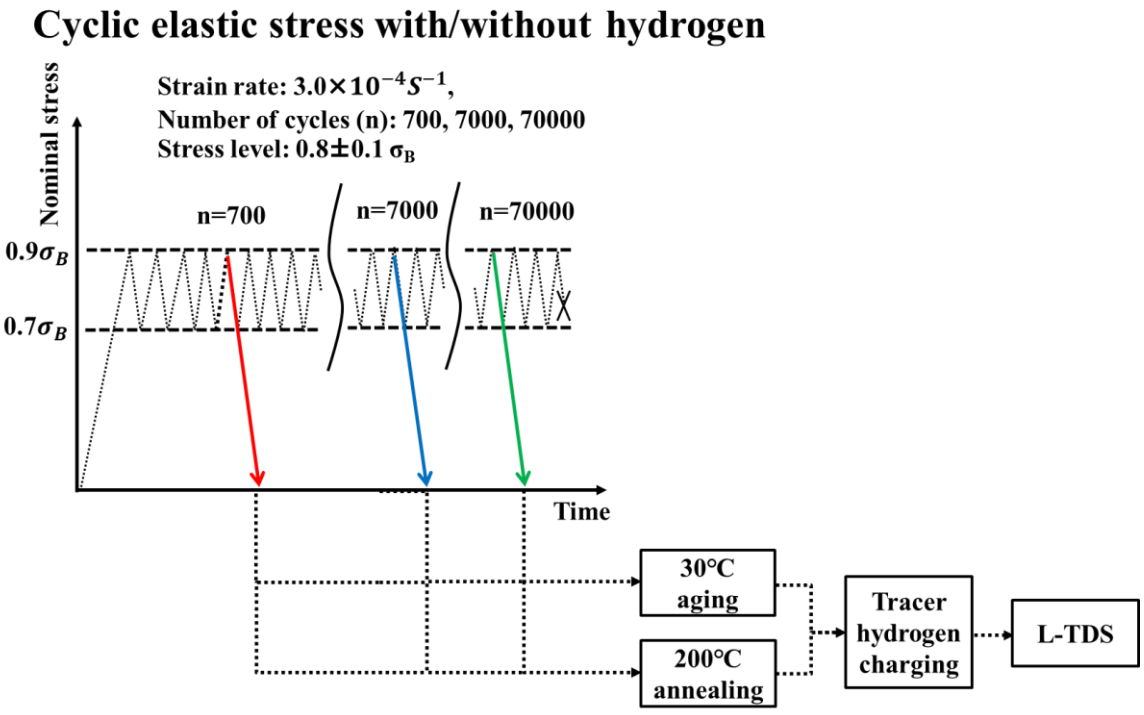

Figure 2. Schematic diagram of the applied cyclic elastic stress and subsequent L-TDS

3 Results

3.1 Tracer hydrogen desorption spectra of the [(n)-cycled] specimens

Figure 3 shows the tracer hydrogen desorption spectra of the [(n)-cycled] specimens, after tracer hydrogen charging under the same conditions as indicated in Section 2.4. The tracer hydrogen of the specimens firstly desorbed at approximately -50 ℃ and disappeared at approximately 60 ℃ in all the tracer hydrogen desorption spectra. The figure shows no significant difference among the specimens

with regard to the states of hydrogen. For the [(n)-cycled] specimens subjected to cyclic elastic stress without hydrogen, the influence of the number of cycles on the states of tracer hydrogen was small.

3.2 Tracer hydrogen desorption spectra of the [H+(n)-cycled] specimen

Figure 4 displays the tracer hydrogen desorption spectra of the [H+(n)-cycled] specimens, after tracer hydrogen charging under the same conditions as indicated in Section 2.4. The tracer hydrogen of the [H+700-cycled] specimen firstly desorbed at approximately -50 °C and disappeared at approximately 60 °C. The tracer hydrogen desorption behavior of the [H+700-cycled] specimen was similar to that of the [(n)-cycled] specimens. However, the tracer hydrogen of the [H+7000-cycled] and [H+70000-cycled] specimens firstly desorbed at approximately -50 °C and disappeared at approximately 100 °C as shown in Figure 4. The disappearance temperature of the tracer hydrogen desorption spectra of the [H+7000-cycled] and [H+70000-cycled] specimens shifted from 60 °C to 100 °C in comparison with that of the [(n)-cycled] specimens. Tracer hydrogen desorption in the high-temperature range from the [H+7000-cycled] and [H+70000-cycled] specimens increased in comparison with that from of the [(n)-cycled] specimens. Additionally, one new peak appeared at approximately 60 °C. These findings indicate that application of cyclic elastic stress in the presence of hydrogen formed new lattice defects with a higher number of cycles.

3.3 Tracer hydrogen desorption spectra of the [H+(n)-cycled+annealed] specimens

Figure 5 depicts the tracer hydrogen desorption spectra of the [H+(n)-cycled+annealed] specimens, after tracer hydrogen charging under the same conditions as indicated in Section 2.4. The tracer hydrogen of the specimens firstly desorbed at approximately -50 °C and disappeared at approximately 60 °C in all the tracer hydrogen desorption spectra. The tracer hydrogen desorption behavior of the [H+(n)-cycled+annealed] specimens was similar to that of the [(n)-cycled] specimens. Tracer hydrogen desorption in the high-temperature range from the [H+(n)-cycled+annealed] specimens was reduced by annealing at 200 °C to the level of the [(n)-cycled] specimens in comparison with that of the [H+(n)-cycled] specimens. These findings indicate that the new lattice defects formed by application of cyclic elastic stress in the presence of hydrogen were annihilated by annealing at a temperature of 200 °C.

3.4 Effects of the number of cycles on tracer hydrogen desorption spectra of three types of specimen

Figure 6 shows the effects of the number of cycles of cyclic elastic stress on the tracer hydrogen contents of the [(n)-cycled], [H+(n)-cycled] and [H+(n)-cycled+annealed] specimens. The tracer hydrogen contents of the specimens were calculated from the area of the tracer hydrogen desorption spectra shown in Figures 3, 4 and 5. The tracer hydrogen contents of the [700-cycled], [7000-cycled] and [70000-cycled] specimens were 0.088, 0.092 and 0.093 mass ppm. The tracer hydrogen contents of the [H+700-cycled], [H+7000-cycled] and [H+70000-cycled] specimens were 0.099, 0.104 and 0.108 mass ppm. The tracer hydrogen contents of the [H+(n)-cycled] specimens increased in comparison with those of the [(n)-cycled] specimens. The tracer hydrogen contents of the [H+700-cycled+annealed], [H+7000-cycled+annealed] and [H+70000-cycled+annealed] specimens were 0.091, 0.094 and 0.096 mass ppm. The tracer hydrogen contents of the [H+(n)-cycled+annealed] specimens were similar to those of the [(n)-cycled] specimens. As shown in Figure 6, the influence of the number of cycles on the tracer hydrogen contents of the [(n)-cycled] and [H+(n)-cycled+annealed] specimens was small. In contrast, the tracer hydrogen contents of the [H+(n)-cycled] specimens increased with an increasing number of cycles.

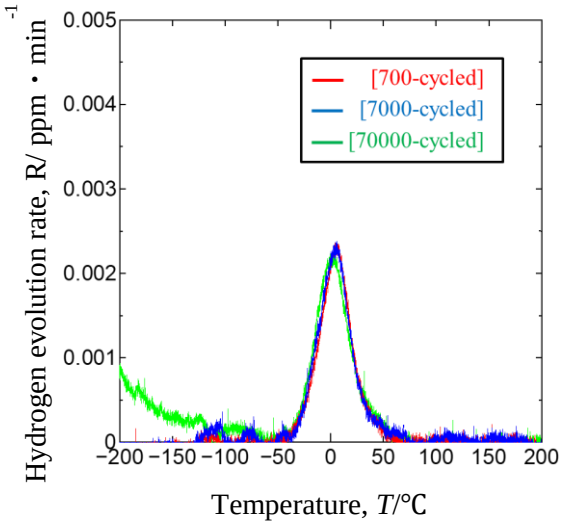

Figure 3. Tracer hydrogen desorption spectra of the [(n)-cycled] specimens

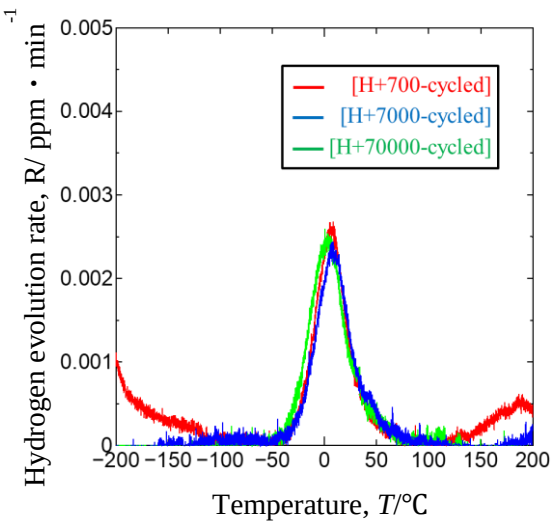

Figure 4. Tracer hydrogen desorption spectra of the [H+(n)-cycled] specimens

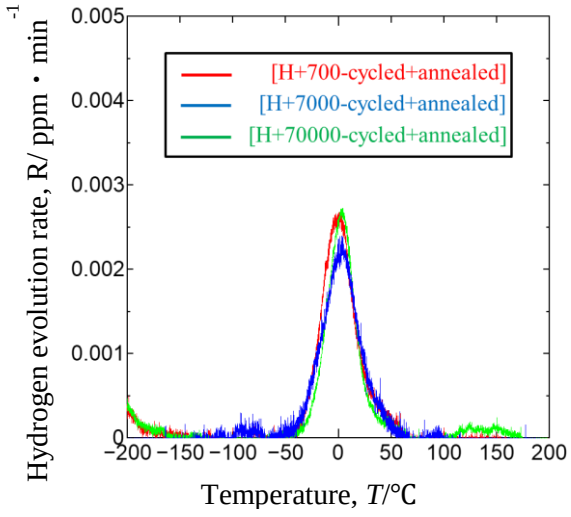

Figure 5. Tracer hydrogen desorption spectra of the [H+(n)-cycled+annealed] specimens

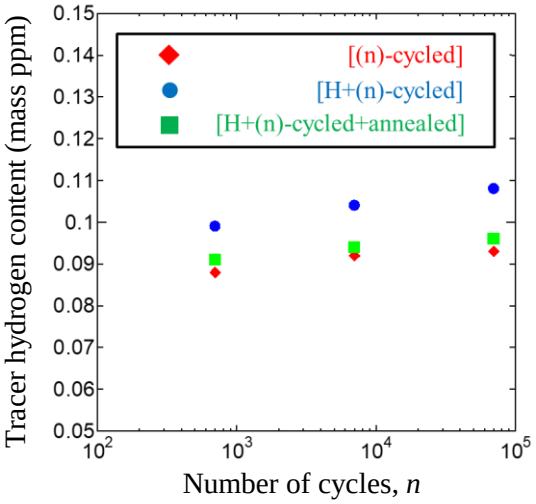

Figure 6. Effects of the number of cycles of cyclic elastic stress on the tracer hydrogen contents of three types of specimens.

4 Discussion

The hydrogen desorption temperature obtained from the tracer hydrogen desorption spectra provides an indication of the binding energy between hydrogen and trapping sites. In addition, the tracer hydrogen content measured by L-TDS provides an indication of the number of lattice defects in steel

when hydrogen is charged until saturation under the same conditions. The tracer hydrogen desorption spectra in Figures 3 and 4 show that tracer hydrogen was desorbed in the high-temperature range from the the [H+(n)-cycled] specimen but not from the [(n)-cycled] specimens. In addition, the tracer hydrogen content of the [H+(n)-cycled] specimens increased in comparison with that of the [(n)-cycled] specimens even though tracer hydrogen charging was carried out until saturation under the same conditions. These findings suggest that changes occurred in the substructure of the tempered martensitic steel specimens during cyclic elastic stress with hydrogen such as the formation and accumulation of lattice defects. However, tracer hydrogen desorption in the high-temperature range from the [H+(n)-cycled+annealed] specimens was annihilated by annealing at a temperature of 200 ℃ as shown in Figure 5. Furthermore, the tracer hydrogen contents of the [H+(n)-cycled+annealed] specimens also decreased to the level of the [(n)cycled] specimens as shown in Figure 6. The tempered martensitic steels used in present study contained dislocations, cementite interfaces and grain boundaries as hydrogen trapping sites. The binding energies between hydrogen and dislocations, cementite interfaces and grain boundaries were 20-30 [5], 19-23 [6] and 10-27 [7] kJ mol^{-1}, respectively. It has also been reported that lattice defects annihilated at 200 °C were vacancy-type defects for medium-carbon steels [8], pure iron [9] and tempered martensitic steel [2]. Taking into consideration of all these factors, it is inferred that the formation of vacancy-type defects was enhanced under the application of cyclic elastic stress in the presence of hydrogen.

5 Conclusions

Changes in the substructure of tempered martensitic steel during the application of cyclic elastic stress in the presence of hydrogen were investigated using L-TDS. The results obtained in this study can be summarized as follows.

(1) The tracer hydrogen desorption behavior of the specimens subjected to cyclic elastic stress without hydrogen showed no significant difference with a higher number of cycles.
(2) Tracer hydrogen desorption in the high-temperature range from the specimens subjected to cyclic elastic stress with hydrogen increased with a higher number of cycles.
(3) Tracer hydrogen desorption in the high-temperature range from the specimens subjected to cyclic elastic stress with hydrogen was reduced by annealing at 200 ℃ to the level of the specimens subjected to cyclic elastic stress without hydrogen. The formation of vacancy-type defects was enhanced under the application of cyclic elastic stress in the presence of hydrogen.

References

[1] Doshida T et al (2012) Enhanced lattice defect formation associated with hydrogen and hydrogen embrittlement under elastic stress of a tempered martensitic steel *ISIJ International* **52.2** 198-207
[2] Saito K et al (2015) *CAMP-ISIJ* **28** 935
[3] Birenis D et al (2018) Interpretation of hydrogen-assisted fatigue crack propagation in BCC iron based on dislocation structure evolution around the crack wake *Acta Materialia* **156** 245-253
[4] Uyama H et al (2006) Effects of hydrogen charge on microscopic fatigue behaviour of annealed carbon steels *Fatigue & Fracture of Engineering Materials & Structures* **29.12** 1066-1074
[5] Hirth JP (1980) Effects of hydrogen on the properties of iron and steel *Metallurgical Transactions A* **11.6** 861-890
[6] Hagi H (1994) Effect of interface between cementite and ferrite on diffusion of hydrogen in carbon steels *Materials Transactions* **35.3** 168-173
[7] Kaneko M et al (2013) *CAMP-ISIJ* **26** 978
[8] Nagumo M et al (2002) Function of hydrogen in intergranular fracture of martensitic steels *Philosophical Magazine A* **82.17-18** 3415-3425
[9] Takai K et al (2008) Lattice defects dominating hydrogen-related failure of metals *Acta Materialia* **56.18** 5158-5167